Journal of Sustainability Science and Management Special Issue Number 1:
The International Seminar on the Straits of Malacca and the South China Sea 2016: 71-80
ISSN: 1823-8556

COASTAL UPWELLING IN THE VICINITY OF TIOMAN ISLAND

ZURAINI ZAINOL AND MOHD FADZIL AKHIR*

Institute of Oceanography and Environment, Universiti Malaysia Terengganu, Terengganu, Malaysia.

**Corresponding author: mfadzil@umt.edu.my*

Abstract: The coastal upwelling in Tioman Island vicinity was studied using the Conductivity, Temperature, Depth sensor (CTD) and Acoustic Doppler Current Profiler (ADCP) data collection and model output during June and August 2014. Different coastal upwelling strength was noted around the island, where the temperature records during the study was on average 0.6 °C cooler at the north (3.1°N latitude) than the south (2.6°N latitude) parts. Slightly high magnitude of increased current speed (~60 cm/s) at the north part of Tioman Island was believed to be the causative factor of the observed temperature difference. Analysis on the vertical section of density and north-south velocity confirmed the separation of current speed in the water column around the island, meanwhile the model simulation of the current circulation during August, 2014 proved the presence of increase current with an average speed of 0.34 m/s around Tioman Island especially at the north of the island.

Keywords: Coastal upwelling, temperature, currents, wind stress, Tioman Island, South China Sea.

Introduction

At the east coast of Peninsular Malaysia (ECPM), seasonally varying wind stress is believed to be an important mechanism in the occurrence of coastal upwelling (Son *et al.*, 2005; Daryabor *et al.,* 2014; Kok *et al.*, 2015). In this region, Akhir *et al.* (2015) had documented the upwelling along the 104 °E longitude and is initiated in June. The cold tongue water started to spread along the ECPM in July and reached its maximum intensity in August while the weakening of upwelling strength occurred in September (Akhir *et al.*, 2015) (Figure 1). Coastal upwelling at ECPM, as reported before (Rojana-anawat *et al.*, 2001; Daryabor *et al.*, 2014; Akhir *et al.*, 2015), brings low temperature and high salinity water towards the surface. Moreover, the isotherms and isohalines uplifting towards the coast was also a good indicator of the presence of upwelling, which was also detected at the ECPM region (Saadon *et al.*, 1997; Kok *et al.*, 2015).

Although the description of ECPM coastal upwelling has been highlighted in few studies (Daryabor *et al.*, 2014; Akhir *et al.*, 2015; Kok *et al.*, 2015), however none of them try to relate the influence of island setting on this feature. Therefore, this research attempt to investigate the coastal upwelling in the vicinity of Tioman Island and its generating factors since numerical study by Jing *et al.* (2009) stated that islands and capes are among the influential factors that induced upwelling. Another question that will be acknowledged in this paper is how Tioman Island circulation influences the upwelling intensity at ECPM. We hypothesized that the presence of Tioman Island in the study area could possibly contribute to the alteration of upwelling strength. This is because, the observation of the average monthly SST (Figure 1) had shown that the water temperature around Tioman Island is slightly cooler than the other area which indicate different upwelling intensity. Moreover, the figure also demonstrates that the cooler upwelled water evolved around Tioman Island (red circles), which could possibly related to island circulation.

Methodology

Study Site

Specifically, the area of interest was limited to Terengganu water and Pahang water extending between 1.7°N – 4.8°N latitude and 103.4°E – 104.4°E longitude along the ECPM with the stations as outlined in Figure 2. A total of 40

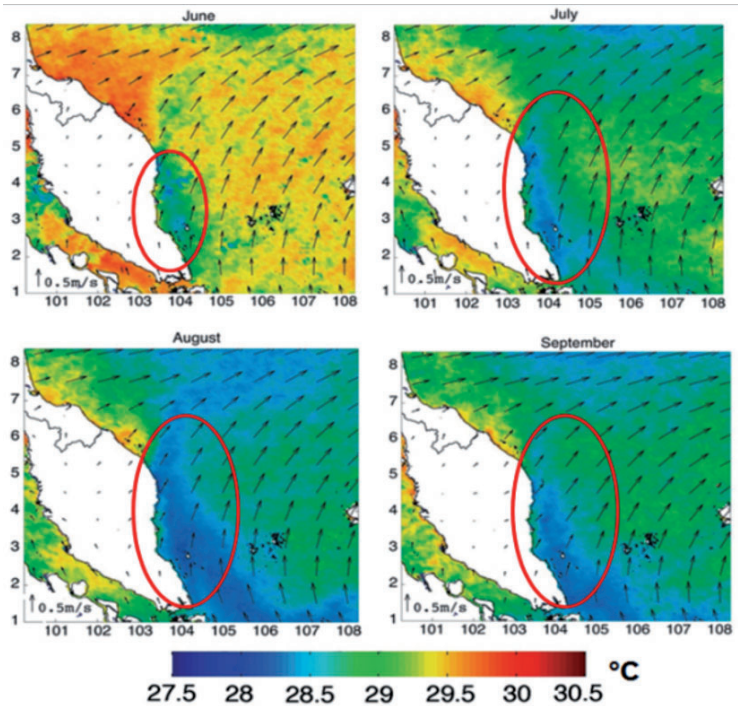

Figure 1: Average monthly MODIS-Terra SST climatology during the southwest monsoon from 2000 – 2012, along with average monthly wind speed (Akhir *et al.*, 2015). The red circles indicate the upwelling event that took place around Tioman Island

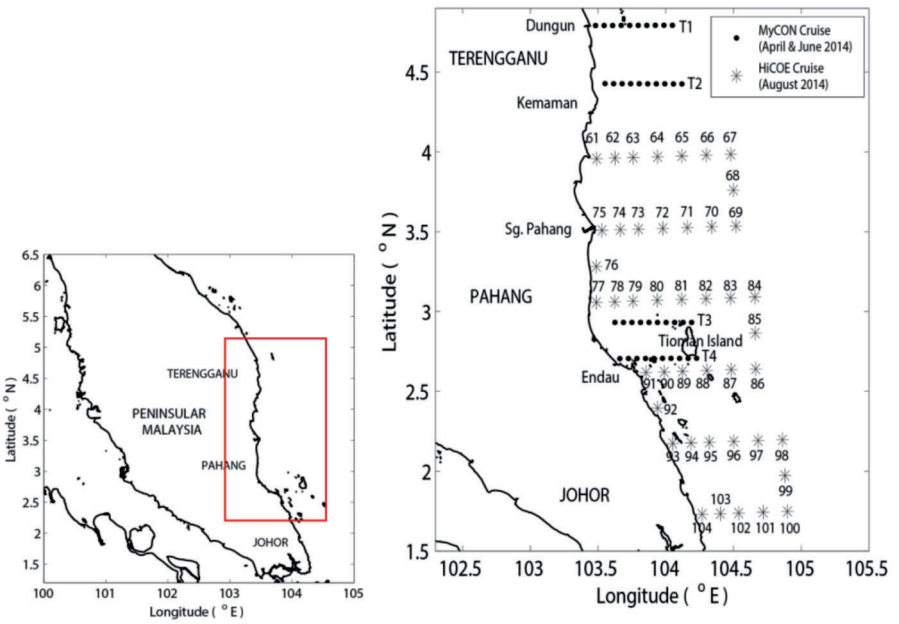

Figure 2: The location of study sites along the east coast of Peninsular Malaysia. The dark filled circle indicates the stations of MyCON cruise during June, 2014 meanwhile the star indicate the stations of HICoE cruise during August 2014

stations (dark filled circles) that were divided into four transects (marked as T1, T2, T3 and T4 in Figure 2) were involved during June 2014 sampling cruise under the Malaysia Coastal Observation Networks (MyCON) project. Unfortunately, due to technical problems, MyCON cruise was replaced by Higher Institution Centre of Excellence (HICoE) in the Marine Science project during August 2014. Although the data from all stations were used to give a general overview of the parameters involved, however this paper also stressed on the characters at the north and south part of Tioman Island specifically at 3.1°N latitude 2.6°N latitude respectively. The sampling was carried out in June (22^{nd} – 26^{th}) and August (18^{th} – 25^{th}) of 2014. In accordance to previous studies by Daryabor *et al.* (2014) and Akhir *et al.* (2015), June and August was chosen since both months represent the upwelling period.

Data Collection and Analysis

In this study, *in-situ* measurement was used as the primary data source, while the model simulation was classified as supporting data. The physical variables of this study were recorded using the SBE Plus19v2 Conductivity, Temperature, Depth (CTD) and Son Tek Acoustic Doppler Current Profiler (ADCP).

In meteorological aspects, the wind data were downloaded from the European Centre for Medium-range Weather Forecast (ECMWF) Interim Reanalysis (ERA Interim) with 0.25° X 0.25° resolution. Changes in upwelling favourable wind conditions were evaluated from the data provided. The daily zonal and meridional wind stress can be calculated by the equations below as defined by Patti *et al.* (2008).

$$\tau_x \text{ (Zonal wind stress)} = \rho_a C_d W_{mag} U \quad \text{Equation 1}$$

$$\tau_y \text{ (Meridional wind stress)} = \rho_a C_d W_{mag} V \quad \text{Equation 2}$$

Where ρ_a is the density of air (1.22 kg/m^3), C_d is the dimensionless drag coefficient (2.6 x 10^{-3}), W_{mag} is the magnitude of wind speed, U is the zonal wind speed and V is the meridional wind speed.

In order to give a clear visualization of the coastal upwelling, the horizontal distribution of temperature was plotted using Ocean Data View (ODV®) software to give a clear image of the parameter at a selected depth. In addition, to further support the result of this study, model simulation of the current circulation around Tioman Island was carried out using MIKE 3 Flow Model by Danish Hydraulic Institute (DHI) Company to examine the relationship between surface currents and coastal upwelling. For the simulation, wind and tidal data was used as the input of the model to generate the current speed and the surface current vectors.

Results

Evidences of Different Upwelling Intensity in Tioman Island Vicinity

The scientific evidence on the presence of the coastal upwelling at ECPM area during the southwest monsoon of 2014 was provided by Zainol & Akhir (In Review). Since the details of the ECPM upwelling was already provided, this chapter will focus on the coastal upwelling in Tioman Island vicinity.

Evidences from the Hydrological Characteristics

In order to show the differences between the characteristic of the north (3.1°N latitude) and south (2.6°N latitude) part of the island during the study, the data obtained from selected stations are compared. The surface temperature values (Table 1) show that the north part of Tioman Island was on average 0.6 °C cooler than the south part with a slight salinity difference (0.2 psu). Evidence for the presence of relatively cooler and saline water at the north part was also obvious at 10-m water depth (Table 2), where the average temperature and salinity difference was 0.4 °C and 0.1 psu respectively. Although the differences in the temperature and salinity values between the north and south part were minimal, however it could be a good indicator of different upwelling strength in Tioman Island vicinity.

Table 1: The surface temperature and salinity around Tioman Island

		Temperature (°C)		Salinity (psu)	
		June	August	June	August
North	S9/81	28.85	29.30	34.38	32.45
	S10/82	29.31	29.00	34.48	32.67
South	S9/88	29.52	29.48	34.33	32.31
	S10/89	29.74	29.75	34.28	32.45

Table 2: The 10-m depth temperature and salinity around Tioman Island

		Temperature (°C)		Salinity (psu)	
		June	August	June	August
North	S9/81	28.52	28.74	34.54	32.59
	S10/82	29.17	28.97	34.50	32.62
South	S9/88	29.34	28.87	34.33	32.53
	S10/89	29.42	28.65	34.38	32.75

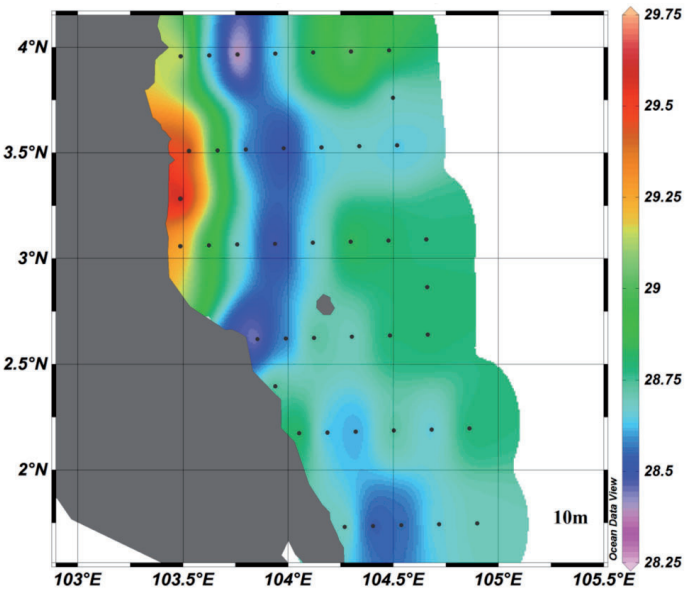

Figure 3: The temperature distribution at 10-m water depth during August 2014 obtained from HICoE cruise

Furthermore, to further prove the differences in Tioman Island vicinity, the temperature distribution at 10-m water depth is presented in Figure 3. From the figure, the cooler water extended along the coast at about 104 °E longitude. Interestingly, around Tioman Island the core of the water mass at the north and south of the island was dominated by the 28.5 °C and 28.7 °C respectively. Therefore, it is proved that the water mass at the north of the island was slightly cooler than the south part with 0.2 °C difference.

Evidences from the Calculated Wind Stress

In this study, the ECMWF wind data were analysed to investigate the influence of coastal winds towards the upwelling at the ECPM.

Therefore, the zonal and meridional wind stress were calculated using the formula as demonstrated in Equations 1 and 2. Figure 4 illustrates the climatological distribution of wind stress in upwelling system at the ECPM during the study period. From the figure, the south-westerly winds blows parallel to the ECPM in high magnitude (exceeding 5.0 m/s) and persistent during the survey period. Besides, the wind stress along the ECPM calculated during the survey trip (August 2014), was positive which indicate an upwelling favourable wind. Specifically near Tioman Island, its position was coincided with the wind stress region of over 0.03 N/m^2 which suggests its important contribution in the upwelling process around the island. This positive wind stress around Tioman Island is believed to be the causative factor that influence the different upwelling intensity around the island.

Evidences from the Current Vectors and Density Profile

The combination of vertical sections of density and north-south ADCP velocity across the

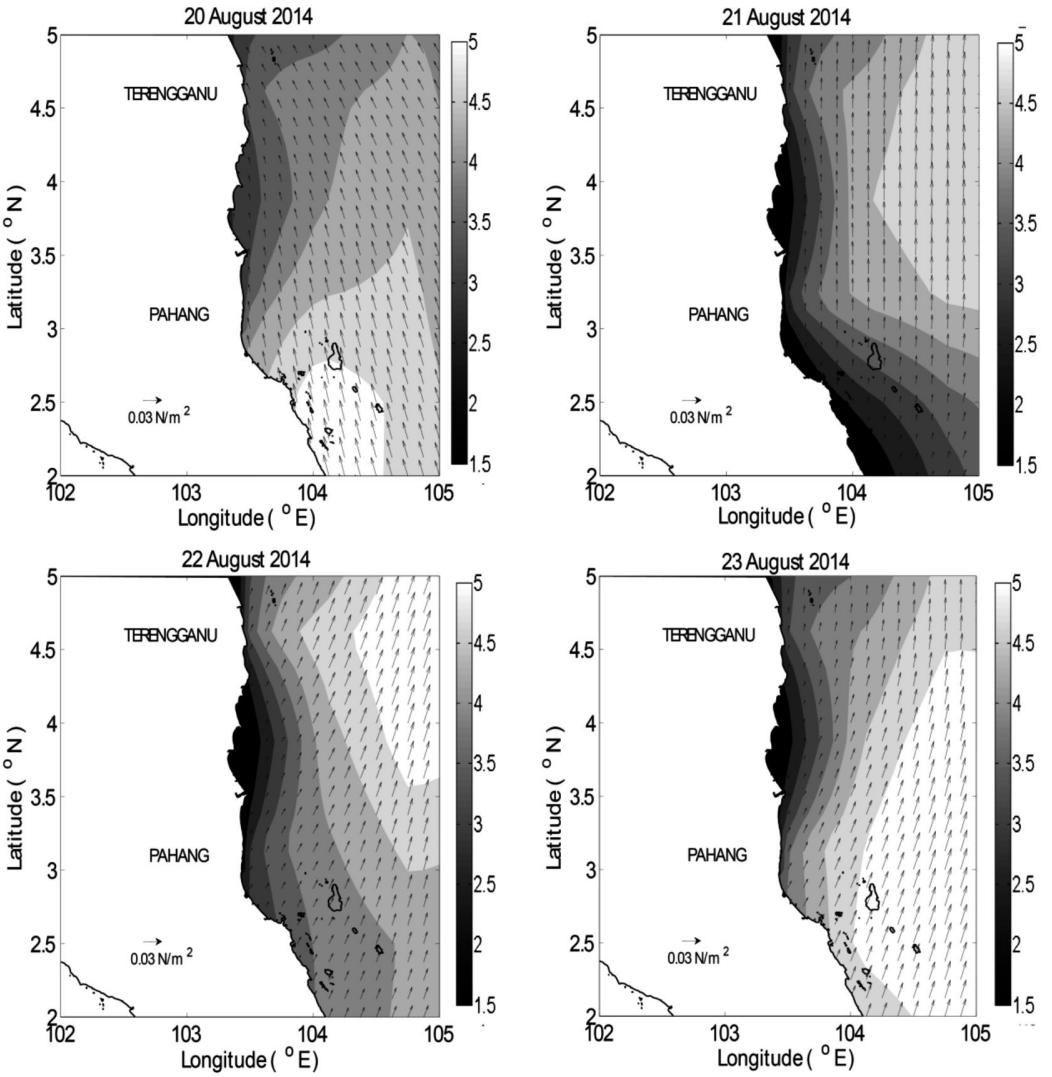

Figure 4: Climatologically wind stress on 20 - 23 August 2014 and magnitude of wind stress (shade in m/s)

Tioman Island transects revealed the different structure of upwelling between these two sections (Figure 5). On the north part of the island, there was a strong pycnocline of 21 kg/m^3 between 20 to 50 m from the upwelling area. However, at the south part, the strong pycnocline only appeared at a depth 30-50 m. This situation was probably due to the north-south velocity of the current where the ADCP speeds were in excess of 60 cm/s in the upwelling area of the north part and reached up to less than 10 m water depth compared to ~20 m at the south part. This strong northward flow was expected as a result of strong western boundary current generated by the southwest monsoon winds, which deflected around Tioman Island. The contribution of this current to the upwelling around the island will be quantified in the discussion part.

Discussion

Description Process of Upwelling in the Vicinity of Tioman Island

The temperature and salinity differences tabulated in Tables 1 and 2 suggested that

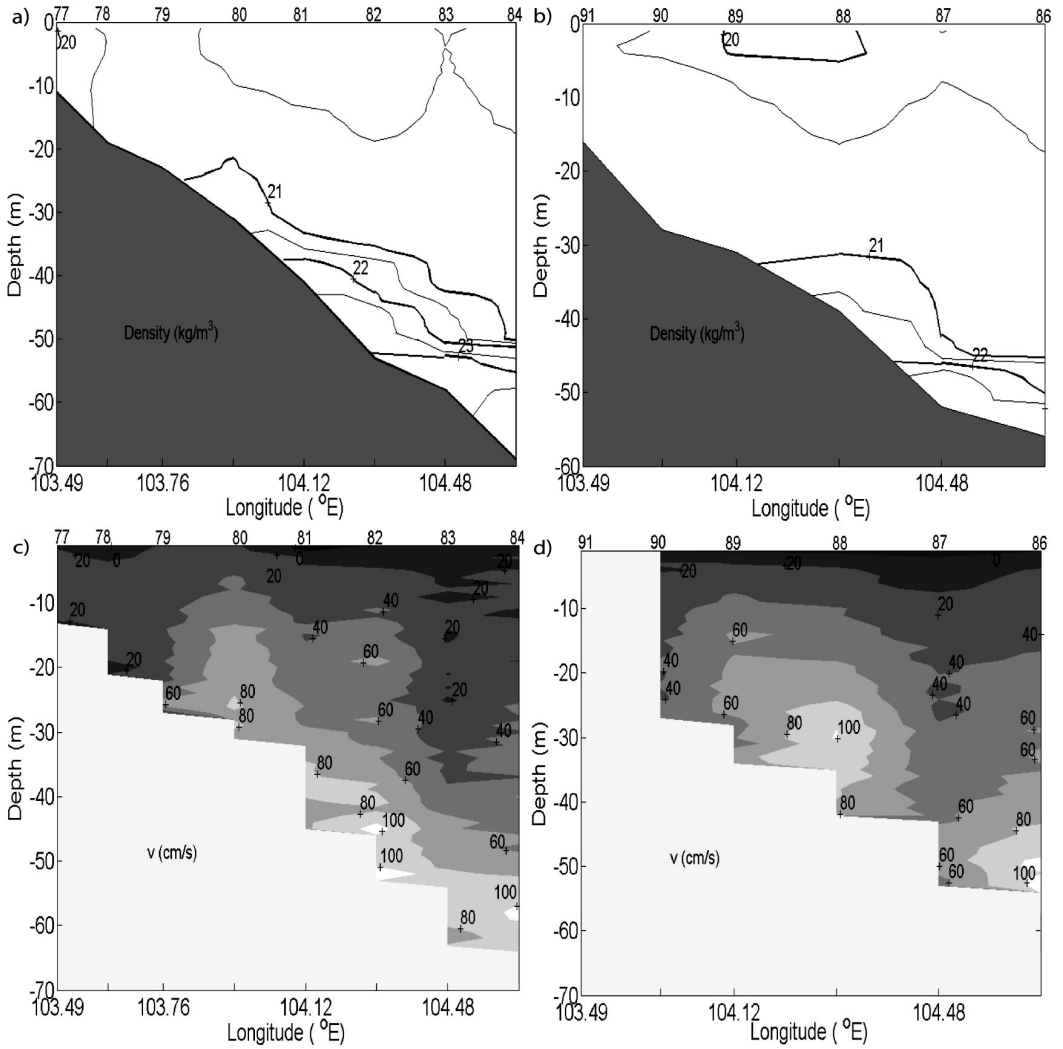

Figure 5: Vertical sections of density and alongshore velocity at the north (a + c) and south (b + d) part of Tioman Island during August 2014

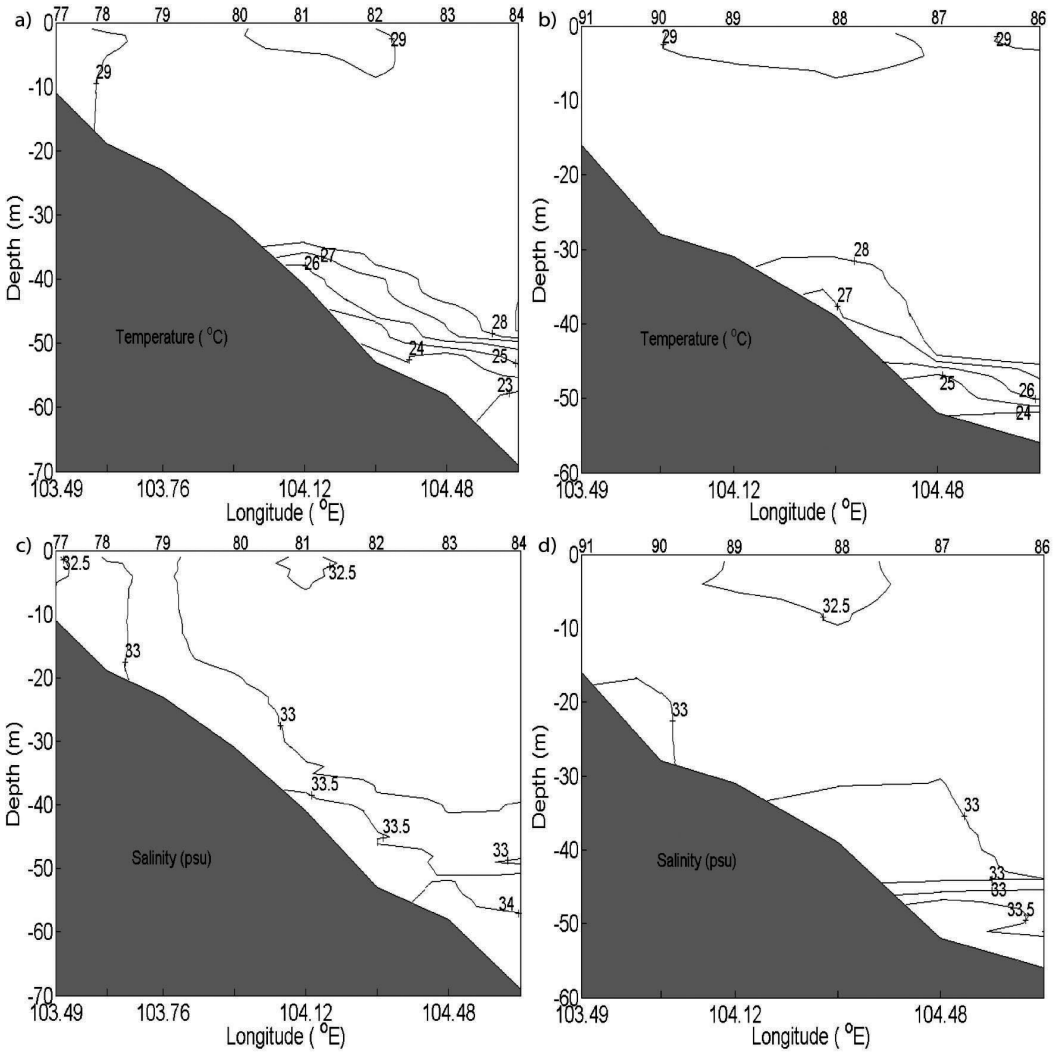

Figure 6: Vertical distributions of temperature (°C) and salinity (psu) during August 2014 at the north (a + c) and south (b + d) part of Tioman Island

the cooler water was more pronounced at the north than the south part of Tioman Island. This situation could indicate that the coastal upwelling at the north of Tioman Island was slightly stronger that the south part. To further illustrate the differences described above, stations 77 - 84 and stations 86 - 91 of HICoE August cruise were selected to represent the north and south part of Tioman Island respectively. Upwelling was evident in both parts of the island, where cooler water shoals up from the deeper layer towards the coast (Figure 6). Interestingly, Figure 6 also demonstrated a vertical uplifting of the 26 °C isotherms to 37 m depth at the north part compared to that about 48 m at the south part of the island, which indicates that the vertical uplifting of the isotherms towards the coast and surface was slightly noticeable at the north than south part of Tioman Island. As mentioned before, this feature is a common sign of upwelling (Akhir *et al.*, 2015) and evidences the presence of upwelling in Tioman Island vicinity.

Although the temperature records during August 2014 were cooler than June 2014, the

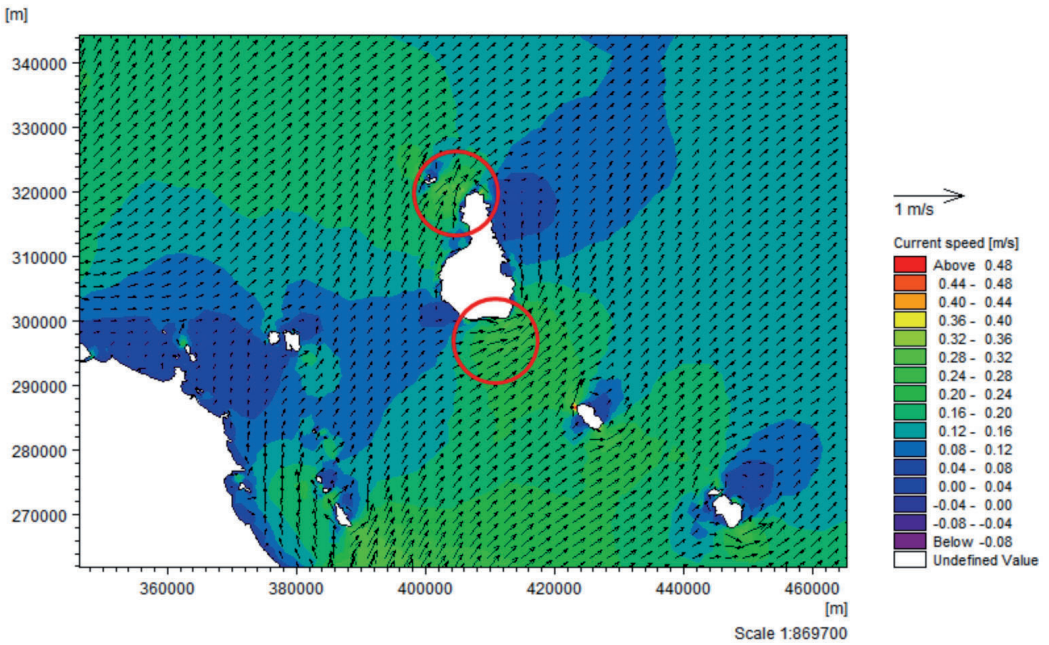

Figure 7: Horizontal distributions of modelled surface current vectors around Tioman Island

opposite situation observed through the salinity data (Table 1 and 2). Less saline water was noted in August 2014 compared to June 2014, which was expected to be under the influence of freshwater intrusion. The low-salinity water that spread in the whole vertical profile during August 2014 (Figure 6) suggests that it may be due to large river discharge, where the geographical location of these stations was situated near to Pahang River. Previous study by Yanagi *et al.* (2001) also suggested the same opinion. However, further quantitative research is required to improve the knowledge gap on how the river discharge does influence the upwelling characteristics especially during August.

Regarding the southwest monsoon winds, the positive wind stress area was consistent with the region of elongated cooler SST and the upwelling region. Similar finding was observed through model simulation in Daryabor *et al.* (2014) where under the absence of wind stress, the elongated cooler SST along ECPM also disappeared meanwhile Barth *et al.* (2000) found a positive relationship between coastal upwelling and seasonal wind stress. The stronger positive wind stress was also recorded on the north part of Tioman Island than the south part which agreed with cooler SST and a stronger flow in this area. Furthermore, the wind stress has been confirmed as one of the important upwelling mechanism at the ECPM in previous literature (Daryabor *et al.*, 2014; Kok *et al.*, 2015). In general, this paragraph managed to illustrate the role of southwest monsoon winds on the coastal upwelling process at the ECPM during the study period through the relationship between positive wind stress and region of cooler SST and strong upwelling .

From the observation of the coastal upwelling process around Tioman Island, increase current speed within an island was also likely took place in this area. Evidence from the *in situ* observation (Tables 1 and 2) and the horizontal distribution of temperature (Figure 3) suggest a strong upwelling to occur at the north part of the island. As mentioned before, this separation was resulted from the strong northward current that was generated by the

upwelling favorable wind, which flows parallel to the coast. To confirm this statement, monthly mean circulation in the study area had been stimulated using MIKE 3 Flow Model software to recognize the strong current location (Figure 7). The model was forced by climatological conditions during the study trip (August 2014). The result of the model simulation clearly demonstrated the increase current speed around Tioman Island, which could be noted at the north and south part of the island. However, in terms of current intensity, the strong current speed off the north of Tioman Island was more apparent. The location of this increase current speed corresponded well with low temperature region of the sub-surface water around Tioman Island (Figure 3). Therefore, the excursion of cooler water in this area most likely associated with the increase current speed around the island.

Conclusion

In conclusion, different coastal upwelling strength in the vicinity of Tioman Island was observed using CTD and ADCP data collection during June and August, 2014. The presence of slightly cooler water at the north of the island than the south part was associated with the local setting of Tioman Island. This difference was believed to be influenced by the current flow around the island and was confirmed using the analysis of the vertical section of density and north-south velocity. Interestingly, the region of positive wind stress around the island was also consistent with this difference. Furthermore, with the presence of the current circulation model simulation during August 2014, the presence of increase current speed around Tioman island especially at the north of the island was proved.

Acknowledgements

The authors wish to thank the staff from Institute of Oceanography and Environment (INOS), Universiti Malaysia Terengganu (UMT) who involved in the 2014 Malaysia Coastal Observation Networks (MyCON) scientific research cruises for their contribution and support. This study was supported by the Research Acculturation Collaborative Efforts (RACE 56011) and Higher Institution Centre of Excellence (HICoE) in Marine Science fund.

References

Akhir, M., Daryabor, F., Husain, M., Tangang, F., & Qiao, F. (2015). Evidence of Upwelling along Peninsular Malaysia during Southwest Monsoon. *Open Journal of Marine Science,* 5: 273-279.

Barth, J., Pierce, S., & Smith, R. (2000). A Separating Coastal Upwelling Jet at Cape Blanco, Oregon and Its Connection to the California Current System. *Deep-Sea Research II,* 47: 783-810.

Daryabor, F., Tangang, F., & Juneng, L. (2014). Simulation of Southwest Monsoon Current Circulation and Temperature in the East Coast of Peninsular Malaysia. *Sains Malaysiana,* 43(3): 389-398.

Jing, Z.-y., Qi, Y.-q., Hua, Z.-l., & Zhang, H. (2009). Numerical Study on the Summer Upwelling System in the Northern Continental Shelf of the South China Sea. *Continental Shelf Research,* 29: 467-478.

Kok, P., Akhir, M., & Tangang, F. (2015). Thermal Frontal Zone along the East Coast of Peninsular Malaysia. *Continental Shelf Research,* 110: 1-30.

Patti, B., Guisande, C., Vergara, A., Riveiro, I., Maneiro, I., Barreiro, A., & Mazzola, S. (2008). Factors Responsible for the Differences in Satellite-based Chlorophyll a Concentration between the Major Global Upwelling Areas. *Estuarine, Coastal and Shelf Science,* 76: 775-786.

Rojana-anawat, P., Pradit, S., Sukramongkol, N., & Siriraksophon, S. (2001). Temperature, Salinity, Dissolved Oxygen and Water Masses of Vietnamese Waters. *Proceedings of the SEAFDEC Seminar on Fishery Resources in the South China Sea, Area IV :*

Vietnamese Waters (pp. 346-355). Samutprakarn, Thailand: Southeast Asian Fisheries Development Center.

Saadon, M. N., Rojana-anawat, P., & Snidvongs, A. (1997). Physical Characteristics of Watermass in the South China Sea, Area I: Gulf of Thailand and East Coast of Peninsular Malaysia. *Proceedings of the First Technical Seminar on Marine Fishery Resources Survey in the South China Sea Area I, Gulf of Thailand and East Coast of Peninsular Malaysia* (pp. 1-5). Bangkok: SEAFDEC.

Son, T., Long, B., & Khin, L. (2005). Main structure of sea surface temperature (SST) in South China Sea from satellite data. *Asian Conference on Remote Sensing (ACRS)* (pp. 1-5). Hanoi: Asian Association on Remote Sensing.

Yanagi, T., Sachoemar, S., Takao, T., & Fujiwara, S. (2001). Seasonal Variation of Stratification in the Gulf of Thailand. *Journal of Oceanography,* 57: 461-470.